Published OnlineFirst August 11, 2009; DOI: 10.1158/1535-7163.MCT-09-0113



# HYD1-induced increase in reactive oxygen species leads to autophagy and necrotic cell death in multiple myeloma cells

Rajesh R. Nair,[1] Michael F. Emmons,[1] Anne E. Cress,[5] Raul F. Argilagos,[1] Kit Lam,[6] William T. Kerr,[2] Hong-Gong Wang,[3] William S. Dalton,[4] and Lori A. Hazlehurst[1,4]

[1]Molecular Oncology, [2]Immunology, [3]Drug Discovery, and [4]Experimental Therapeutics Programs, Moffitt Cancer Center, Tampa, Florida; [5]Department of Cell Biology and Anatomy, University of Arizona, Tucson, Arizona; and [6]Internal Medicine, University of California Davis, Davis, California

## Abstract

**HYD1 is a D–amino acid peptide that was previously shown to inhibit adhesion of prostate cancer cells to the extracellular matrix. In this study, we show that in addition to inhibiting adhesion of multiple myeloma (MM) cells to fibronectin, HYD1 induces cell death in MM cells as a single agent. HYD1-induced cell death was necrotic in nature as shown by: (*a*) decrease in mitochondrial membrane potential ($\Delta\psi_m$), (*b*) loss of total cellular ATP, and (*c*) increase in reactive oxygen species (ROS) production. Moreover, HYD1 treatment does not result in apoptotic cell death because it did not trigger the activation of caspases or the release of apoptosis-inducing factor and endonuclease G from the mitochondria, nor did it induce double-stranded DNA breaks. HYD1 did initiate autophagy in cells; however, autophagy was found to be an adaptive response contributing to cell survival rather than the cause of cell death. We were further able to show that *N*-acetyl-L-cysteine, a thiol-containing free radical scavenger, partially protects MM cells from HYD1-induced death. Additionally, *N*-acetyl-L-cysteine blocked HYD1-induced as well as basal levels of autophagy, suggesting that ROS can potentially trigger both cell death and cell survival pathways. Taken together, our data describe an important role of ROS in HYD1-induced necrotic cell death in MM cells. [Mol Cancer Ther 2009;8(8):2441–51]**

## Introduction

Despite recent advances in the treatment of multiple myeloma (MM), the disease remains incurable. There is accumulating evidence that targeting multiple cell death pathways may be an advantageous strategy for treating cancers, such as MM, which are currently not cured by standard therapy that targets the apoptotic pathway (for review, see ref. 1). Cell death in mammalian cells can be broadly classified into three types. Morphologically, type I cell death (apoptosis) is characterized by chromatin condensation and DNA fragmentation, type II cell death (autophagy) is characterized by a massive accumulation of double-membrane vesicles commonly referred to as autophagosomes, and type III cell death (necrosis) is characterized by oncosis and plasma membrane rupture (2). Although all three types have been shown to undergo a sequential programmed cell death mechanism, the majority of conventional anticancer therapeutic agents used in hematologic malignancies use the apoptotic pathway to induce cell death (for review, see ref. 3). Unfortunately, during progression toward drug-resistant disease, the apoptotic machinery, consisting of antiapoptotic and proapoptotic proteins, is not balanced and often favors cell survival after cytotoxic insult. In such a scenario, agents that initiate nonapoptotic cell death may easily overcome the inherent deficiencies of the apoptotic machinery in cancer cells. As a result, targeting alternative cell death pathways may represent an attractive approach to increasing overall tumor cell kill.

Necrosis is often defined as a default cell death pathway. This concept is supported by evidence that in mouse embryonic fibroblasts and in immortalized baby mouse kidney epithelial cells, overexpressing antiapoptotic protein Bcl-2, or simultaneous knockdown of proapoptotic proteins Bax or Bak (apoptotic pathway) and depletion of beclin-1 (autophagic pathway), leads to necrotic cell death when exposed to hypoxia or etoposide (4, 5). In terms of biochemical changes, loss of mitochondrial membrane potential ($\Delta\psi_m$) is considered a hallmark feature of necrotic cell death. Loss of $\Delta\psi_m$ has been attributed to be a response to an increase in cytosolic free calcium, anoxia, and overproduction of reactive oxygen species (ROS; for review, see ref. 6). Although both apoptosis and necrosis require $\Delta\psi_m$ loss, the distinguishing difference between the two is that in necrosis, $\Delta\psi_m$ loss is accompanied by a total cellular loss in ATP, which is maintained and required for apoptosis (7).

In the present study, we show that HYD1 (kikmviswkg), a peptide containing 10 D–amino acids previously reported to block cell adhesion to the matrix in epithelial prostate

Received 2/10/09; revised 5/28/09; accepted 6/8/09; published OnlineFirst 8/11/09.

**Grant support:** National Cancer Institute grant R01CA122065 and the Multiple Myeloma Research Foundation (L.A. Hazlehurst). Supported in part by the Flow Cytometry Core facility at the H. Lee Moffitt Cancer Center & Research Institute, a comprehensive cancer center designated by the NCI.

The costs of publication of this article were defrayed in part by the payment of page charges. This article must therefore be hereby marked *advertisement* in accordance with 18 U.S.C. Section 1734 solely to indicate this fact.

**Note:** Supplementary material for this article is available at Molecular Cancer Therapeutics Online (http://mct.aacrjournals.org/).

R.R. Nair and M.F. Emmons contributed equally to the manuscript.

**Requests for reprints:** Lori Hazlehurst, Molecular Oncology, H. Lee Moffitt Cancer Center, Tampa, FL 33613. Phone: 813-903-6807; Fax: 813-979-7265. E-mail: Lori.Hazlehurst@moffitt.org



doi:10.1158/1535-7163.MCT-09-0113

Published OnlineFirst August 11, 2009; DOI: 10.1158/1535-7163.MCT-09-0113



carcinoma cells (8), can induce cell death in H929, 8226, and U266 MM cell lines but not in CD34+ hematopoietic progenitor cells or peripheral blood mononuclear cells. The induction of cell death is distinct from apoptosis and autophagy, and is associated with the loss of $\Delta\psi_m$, ATP depletion, and the induction of ROS. Furthermore, HYD1-induced necrotic cell death was partially reversible by pretreatment with *N*-acetyl-L-cysteine. Paradoxically, increased ROS in HYD1-treated cells results in the induction of autophagy, which protects cells against HYD1-induced necrotic cell death. In summary, these data provide rationale for further preclinical development of HYD1 and HYD1 derivatives that preferentially target alternative cell death pathways.

## Materials and Methods

### Cell Culture

H929, 8226, and U266 cells were obtained from the American Type Culture Collection and maintained at 37°C in 5% $CO_2$/95% air atmosphere. Cells were grown in suspension in RPMI 1640 (Cellgro; Fischer Scientific) supplemented with fetal bovine serum (Omega Scientific; 10% in H929 and U266 cells, and 5% in 8226 cells), penicillin (100 μg/mL), streptomycin (100 μg/mL), and 2 mmol/L L-glutamine (Life Technologies). For H929 cells, 0.05 mmol/L 2-mercaptoethanol was added to the culture media.

### Chemical Reagents, Antibodies, and Peptides

5-(and-6)-carboxy-2′,7′-dichlorodihydrofluorescein diacetate, 5-chloromethylfluorescein diacetate, and 3,3′-dihexyloxacarbocyanine iodide were purchased from Invitrogen. Tunicamycin, melphalan, *N*-acetyl-L-cystein, *tert*-butyl hydroperoxide, and 3-methyladenine were purchased from Sigma Aldrich. Recombinant soluble KillerTRAIL was purchased from Alexis Biochemicals. zVAD-fmk pan caspase inhibitor was purchased from BD Biosciences. Anti–α4 integrin (clone P4G9) was purchased from Abcam, anti–α5 integrin (clone P1D6) was purchased from Calbiochem, and anti–β1 integrin (AIIB2) was a generous gift of Dr. Anne Cress. Anti–topoisomerase IIβ was purchased from BD Biosciences; anti-Bax (N20) from Santa Cruz Biotechnologies; anti–LC-3 and anti–endonuclease G from Novus Biologicals; and anti–β-actin, anti-Bax (6A7), and anti–α-tubulin from Sigma Aldrich. Anti–caspase-8, anti–caspase-9, anti–caspase-3, anti–Beclin-1, and anti–apoptosis-inducing factor were purchased from Cell Signaling. HYD1 (kikmviswkg) and HYDS (wiksmkivkg) D–amino acid peptides were synthesized by Global Peptides.

### Quantification of Cell Adhesion to Fibronectin

Briefly, H929 myeloma cells were preincubated with varying concentrations of either HYD1 or the scrambled peptide (HYDS) for 30 min before allowing cells to attach to fibronectin for 2 h. Cell adhesion was detected by crystal violet staining as previously described (9, 10).

### Quantification of Cell Adhesion to HS-5 Bone Marrow Stroma Cells

Adhesion of H929 cells to the HS-5 bone marrow stroma cell line was done as previously described (11).

### Coculture Model of Drug Resistance

HS-5 ectopically expressing green fluorescent protein (GFP) were plated at a density of 200,000 cells/mL overnight in a 6-well plate. The following day, H929 cells at a density of 200,000 cells were incubated for 30 min with either 50 μg/mL HYDS, HYD1, or vehicle control (ddH20), and then added to HS-5 cells. H929 cells were allowed to adhere for 3 h before the addition of 15 μmol/L melphalan to appropriate samples. Cell death was measured 24 h later with the use of Annexin V–phycoerythrin (PE) staining. Positive GFP–expressing events were gated out of the analysis.

### Cell Death Analysis

Cells were washed with an Annexin V binding buffer (BioVision Inc.) and incubated with either Annexin V–PE or a combination of Annexin V–FITC/propidum iodide (PI). The cells were then analyzed for fluorescence with the use of FACScan (BD Biosciences). Caspase-3 and caspase-8 activity was measured at 6 and 24 h post peptide treatment per manufacturer's instructions (BD Biosciences).

### Clonogenic Assay

H929 cells were treated with HYD1 for 2 h and then diluted to 0.3% final agar solution reconstituted in growth media, and then dispersed in triplicate in 35-mm culture plates containing 2,500 cells in each plate. Once the agar solidifies, cells were allowed to incubate for 12 additional days. Cell colonies (>50 cells) were then counted on 2-mm grid culture dish (Corning).

### Colony Formation Assay

Whole blood from healthy donors was used to isolate CD34+ hematopoeitic progenitor cells with the aid of a CD34 MicroBead kit (Miltenyi Biotec Inc.). The CD34+ cells were then washed and resuspended in Incomplete MethoCult media supplemented with 2% fetal bovine serum and treated for 2 h with HYD1 (StemCell Technologies). The cells were then diluted in MethoCult (StemCell Technologies) and then dispensed in duplicate 35-mm culture plates containing 5,000 cells in each plate. Colonies were scored on day 12.

### Immunoprecipitation

After treatment, cells were lysed, and 500 μg of cell lysate were incubated overnight with anti-Bax (6A7) at 4°C. After incubation, lysates were further incubated with 25 μL of protein A/G agarose beads for 2 h. The lysate mixture was then washed thrice with CHAPS lysis buffer, and the immunoprecipitated proteins were then subjected to Western blotting as described below. Anti-Bax (N20) antibody was used to probe for Bax protein.

### Neutral Comet Assay

Cells were treated with either 50 μg/mL HYD1, HYDS, or 50 ng/mL tumor necrosis factor–related apoptosis-inducing ligand for 6 h. After drug treatment, 5,000 cells were pelleted and resuspendend in PBS agar solution, and overlayed onto fully frosted glass slides. The neutral comet assay was done as previously described by our laboratory (12).

### Western Blotting

Cells were plated in a 6-well plate at a concentration of 400,000 cells/mL. After treatment, cells were placed on ice and lysed in 100 μL of cold lysis buffer [120 mmol/L NaCL,

Published OnlineFirst August 11, 2009; DOI: 10.1158/1535-7163.MCT-09-0113



50 mmol/L Tris-HCL (pH 7.6), 0.5% NP40, 1 mmol/L EDTA, 1 mmol/L $Na_3VO_4$, 1 mmol/L phenylmethylsulfonyl fluoride, and 1 μg/mL aprotinin and leupeptin]. Total protein (10 μg) was applied to an 8% SDS-PAGE gel. Proteins were resolved by electrophoresis and then transferred to a polyvinylidene difluoride membrane.

### Electron Microscopy

H929 cells were treated for 4 h with either 50 μg/mL HYD1 or HYDS. After peptide treatment, samples were fixed overnight in 2.5% glutaraldehyde in 0.1 mol/L phosphate buffer (pH 7.2) at 4°C. After fixation and dehydration with acetone, samples were suspended in 1:1 mixture of 100% acetone–embedding medium for 1 h while under vacuum. Thin sections (80-90 nm) were picked up on 100-mesh copper grids, stained with 8% aqueous uranyl acetate for 10 min, and Reynolds lead citrate for 5 min. Thin sections were examined with a Philips CM10 transmission electron microscope at 60 kV. Representative cells were photographed, printed, and scanned.

### Small Interfering RNA Transfection

Transfection of H929 cells was done as previously described (13). Briefly, 3.5 million H929 cells were added to 200 μL of cytomix buffer (pH 7.6) containing 120 mmol/L KCl, 0.15 mmol/L $CaCl_2$, 10 mmol/L $K_2HPO_4/KH_2PO_4$, 25 mmol/L HEPES, 2 mmol/L EGTA, 5 mmol/L $MgCl_2$, 2 mmol/L ATP, 5 mmol/L glutathione, and 1.25% DMSO. Ten microliters of a 20-μmol/L stock small interfering RNA directed at Beclin-1 (Dharmacon) or nonsilencing (Dharmacon) was added to the buffer. The mixture was placed in a 2-mm cuvette, and electroporation was done at 140 V/975 μF. After transfection, cells were incubated in the buffer for 15 min at 37°C. The mixture was transferred to a 25-mL flask containing 10 mL of fresh media. Cells were incubated for an additional 72 h before treatment with HYD1.

### Measurement of ROS

Cells were suspended in prewarmed PBS containing 5 μmol/L of 5-(and-6)-carboxy-2′,7′-dichlorodihydrofluorescein diacetate for 20 min. The cells were then washed to remove the unloaded dye, returned to prewarmed growth media, and further incubated for 30 min. During the recovery period, when indicated, cells were treated with *N*-acetyl-L-cysteine (10 mmol/L). The cells were treated as indicated, and the fluorescence intensity was analyzed with the use of Wallace VICTOR$^2$ 1420 multilabel counter (EG&G Wallace; excitation: 485 nm; emission: 535 nm).

### Measurement of $\Delta\psi_m$

After treatment, cells were incubated for 15 min with 15 nmol/L of 3,3′-dihexyloxacarbocyanine iodide (Molecular Probes, Invitrogen). Cells were washed with PBS and resuspended in 500 μL of PBS, and the loss of $\Delta\psi_m$ in cells was then analyzed with the use of FACScan (BD Biosciences)

### ATP Measurement

Treated cells were lysed in radioimmunoprecipitation assay buffer (Upstate), and ATP concentrations were measured with the use of ENLITEN ATP assay system bioluminescence detection kit as per manufacturer's instructions (Promega). The ATP concentration was later normalized to the protein content of the lysates.

### SCID-Hu Model

The SCID-Hu model was done as previously described (14). Briefly, SCID/beige mice 4 to 6 wk old were purchased from Taconic. Fetal tissue (18-23 wk) was obtained from Advance Bioscience Resources in compliance with state and federal government regulations. Two bones were surgically implanted in the mammary fat pad of 6-to-8-week-old female SCID mice. After 6 wk of bone engraftment, 50,000 H929 cells were injected directly into the bone, and tumor was allowed to engraft for 4 wk. At 28 d, baseline tumor burden was quantified in the sera with the use of a κ ELISA kit per manufacturer's instructions (Bethyl), and mice were randomized into treatment groups. HYD1 mice were treated with 8 mg/kg (i.p.) daily as indicated for 21 d. Tumor burden was assessed weekly by measuring κ levels in the sera.

### Statistical Analysis

Experiments were independently done thrice unless specified otherwise in the legend. The data were plotted as mean ± SD and analyzed for statistical significance between treatment groups with the use of ANOVA followed by post hoc Student-Newman-Keuls test. For the dose-response curves depicted in Figs. 4C and 5B, a paired *t* test was used to test for comparisons between treatment groups. For the *in vivo* study, the data were plotted as mean ± SD and analyzed for statistical significance with the use of repeated-measures ANOVA. A $P < 0.05$ was accepted as statistically significant.

## Results

### HYD1 Blocks Adhesion to Fibronectin, Induces Cell Death in MM Cells *In vitro*, and Reverses Resistance Associated with the Bone Marrow Stroma Coculture Model

HYD1 was previously shown to inhibit integrin-dependent cell adhesion in epithelial prostate carcinoma (8, 15). Similarly, in this study we show that HYD1 blocks α4β1-mediated adhesion of MM cells to fibronectin (see Fig. 1A). In contrast, HYD1 did not block MM cell adhesion to bone marrow stroma cells, a finding that was consistent with a β1-blocking antibody (see Fig. 1B), suggesting that multiple cell adhesion molecules regulate adhesion of MM cells to bone marrow stroma. We postulated that if β1 integrin and not cell attachment were important in conferring drug resistance, then HYD1 treatment should reverse resistance associated with the coculture model. As shown in Fig. 1C, HYD1 treatment reduced the level of resistance to melphalan in the bone marrow stroma coculture model system, a finding that was more dramatic in 8226 cells compared with H929 cells (see Fig. 1C and Supplementary Fig. S1). Upon testing HYD1 in the coculture model system, an unanticipated observation was that HYD1 treatment induced cell death in suspension cultures as a single agent. Furthermore, MM cells were not resistant to HYD1 in the context of the coculture model (see Fig. 1D). Finally, HYD1 increased the levels of melphalan-specific cell death in both suspension and coculture conditions.

Published OnlineFirst August 11, 2009; DOI: 10.1158/1535-7163.MCT-09-0113



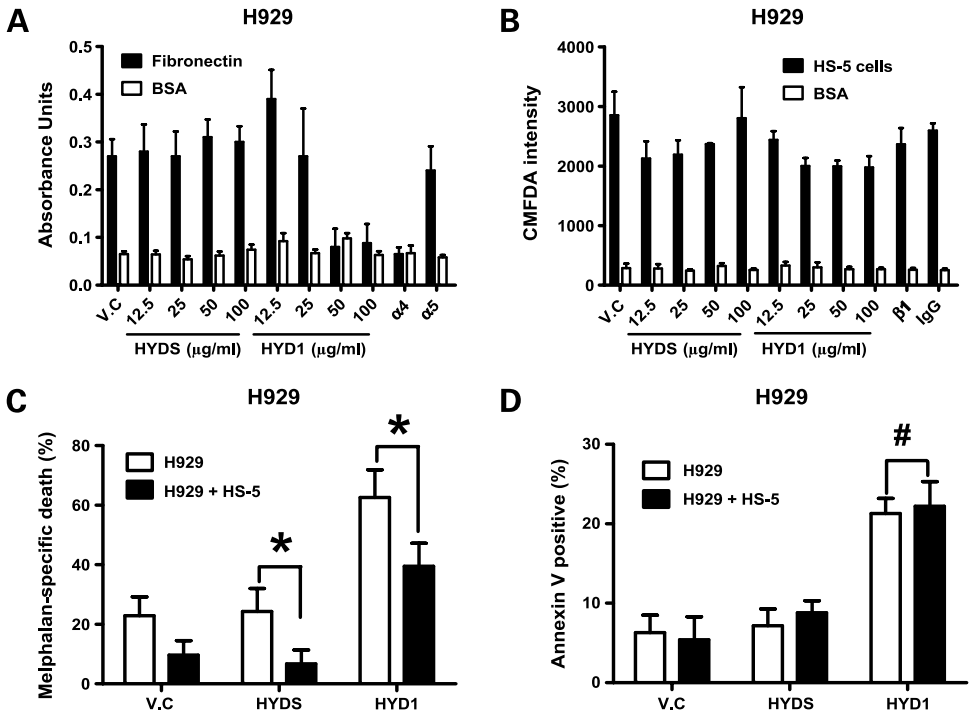


**Figure 1.** HYD1 blocks α4β1-mediated cell adhesion, and induces equivalent cell death in suspension and in the HS-5 bone marrow stroma coculture model. **A,** H929 cells were pretreated for 30 min with varying doses of HYD1 or 1:100 dilution of α4-blocking or α5-blocking antibody as described in Materials and Methods. Shown is a representative of three independent experiments done in quadruplicate. **B,** H929 cells were loaded with CMFDA as described in Materials and Methods, and cells were pretreated with varying concentrations of HYD1 or a 1:100 dilution of β1-blocking antibody. Shown is a representative of three independent experiments done in quadruplicate. **C,** coculture model of drug resistance was studied in H929 cells as described in Materials and Methods. Melphalan-specific cell death was calculated by subtracting out baseline death observed in control, HYD1-treated, and HYDS-treated cells. Thus, HYD1 melphalan-specific death = % Annexin V–positive melphalan + HYD1 treatment - % Annexin V–positive in HYD1 treatment only. HYDS melphalan-specific death = % Annexin V–positive melphalan + HYDS treatment - % Annexin V–positive HYDS ($n = 9$; *, $P < 0.05$). **D,** H929 cells were pretreated for 30 min with 50 μg/mL HYD1 before either growth in suspension or as a coculture. Twenty-four hours after drug treatment, Annexin V staining and FACS analysis were used to detect dead MM cells ($n = 9$; #, $P > 0.05$). CMFDA, 5-chloromethylfluorescein diacetate; FACS, fluorescence-activated cell sorting.

Due to the finding that HYD1 induced equivalent cell death in MM cells as a single agent in both suspension cultures and in the coculture model, we decided to further investigate the mechanism of action of HYD1-induced cell death in suspension cultures. MM cells were treated with 12.5 or 50 μg/mL of HYD1, or the scrambled peptide control HYDS, for 6 hours followed by measurement of Annexin V–positive cells, used as a marker for cell death. As shown in Fig. 2A, HYD1 treatment increased Annexin V–positive cell staining compared with cells treated with the scrambled variant HYDS in H929 cells. Additionally, as shown in Fig. 2B, HYD1 inhibited in a dose-dependent manner the ability of H929 cells to form colonies in soft agar. HYD1 was also found to induce cell death in 8226 and U226 cells (see Fig. 2C and D).

### HYD1 Does Not Induce Apoptotic Cell Death

To examine if HYD1-induced cell death was dependent on the apoptotic pathway involving caspases, we investigated the processing and activation of caspases. As seen in Fig. 3A, 6-hour treatment with 50 μg/mL of HYD1 did not result in the activation of caspase-8 and resulted in only a minimal activation of caspase-3. Also, HYD1 treatment did not give rise to cleaved active forms of caspase-3, caspase-9, and caspase-8, as ascertained by Western blot analysis in H929 cells (Fig. 3B). The absence of cleaved caspases was also observed in 8226 cells (Supplementary Fig. S2). Endonuclease G and apoptosis-inducing factor, depending on the cellular context and cytotoxic insult, have been reported to be released from the mitochondria in both a caspase-dependent and a caspase-independent manner (16, 17). Pro-apoptotic protein Bax has been implicated in the formation of outer membrane mitochondrial pore, causing the release of apoptosis-inducing factor and endonuclease G from the mitochondria. This is followed by translocation of apoptosis-inducing factor and endonuclease G to the nucleus, leading to DNA fragmentation and nuclear condensation (18). To first investigate whether HYD1 caused a conformational change in Bax, we did immunoprecipitation to pull down the active form of Bax (19). As shown in Fig. 3C, HYD1 treatment failed to increase the proportion of active Bax because the levels were comparable with those seen in HYDS-treated and control cells. We followed this study by doing a cellular enrichment of treated cells into the nuclear and the cytosolic fractions. As shown in Fig. 3C, no translocation of

Published OnlineFirst August 11, 2009; DOI: 10.1158/1535-7163.MCT-09-0113



apoptosis-inducing factor or endonuclease G from the cytoplasm to the nucleus was observed after 6-hour treatment with HYD1. These data indicate that HYD1 treatment does not lead to cell death through a caspase-independent translocation of endonuclease G and apoptosis-inducing factor from the mitochondria to the nucleus. Finally, double-stranded DNA breaks resulting from the internucleasomal DNA cleavage by endonucleases (mediated predominately by caspase-activated DNase, lysosomal DNase II, and endonuclease G) are important biochemical markers for apoptotic cell death (20). To determine if double-stranded breaks are involved in HYD1-induced cell death, H929 cells were treated for 6 hours with HYD1 and then subjected to neutral comet assay. Tumor necrosis factor–related apoptosis-inducing ligand was used as a positive control for apoptotic cell death. As seen in Fig. 3D, tumor necrosis factor–related apoptosis-inducing ligand treatment lead to a significant increase in comet moments. However, HYD1, HYDS, and control cells showed equivalent comet moments, indicating the absence of activation of endonucleases and double-stranded DNA breaks in HYD1-treated cells.

Finally, we determined whether HYD1 induced a latent induction of caspases. The pan caspase inhibitor zVAD-fmk was used to determine whether caspases contributed to HYD1-induced cell death after 24 hours of HYD1 treatment. As shown in Supplementary Fig. S3, pretreatment of H929 cells with zVAD-fmk did not inhibit cell death induced by HYD1. In contrast, zVAD-fmk treatment blocked the majority of the melphalan-treated Annexin V–positive cells. Of note with HYD1 treatment, PI and Annexin V positivity occur simultaneously, which is not the case for melphalan treatment, in which you can observe a predominant Annexin V–positive and PI-negative cell population. These data were consistent with caspase activity assays, which showed that neither caspase-3 nor caspase-8 activity was induced after 24 hours of HYD1 treatment (see Supplementary Fig. S3). Taken together, these data show that HYD1-induced cell death occurs independent of caspase and endonuclease activity, indicating that HYD1 does not induce apoptosis in MM cells.

### HYD1 Induces Autophagy in MM Cells

We used electron microscopy to observe the morphology of HYD1-treated cells. As shown in Fig. 4A, 4-hour treatment with HYD1 in H929 cells revealed the presence of several autophagosomes, observed as extensive double-membrane vacuolar structures containing cytoplasmic contents. Such autophagosomes were absent in HYDS-treated cells. Another hallmark of autophagy is the lipidation of LC3 protein, which can be detected by Western blot analysis (21). Thus, we did Western blot analysis to determine whether HYD1 treatment caused the conversion of the cytoplasmic form of LC3 (LC3-I, 18 kDa) to the autophagosomal membrane–bound form of LC3 (LC3-II, 16 kDa). As seen in Fig. 4A, and consistent with the electron microscopy data, 4-hour treatment with HYD1 and tunicamycin, a known inducer of autophagy, resulted in increased conversion of LC3-I to LC3-II. Additional markers of autophagy include an increase in the formation of acidic vesicles. As shown in Supplementary Fig. S4, HYD1 treatment caused an increase in the number and size of acidic vesicles, as shown by LysoSensor staining.

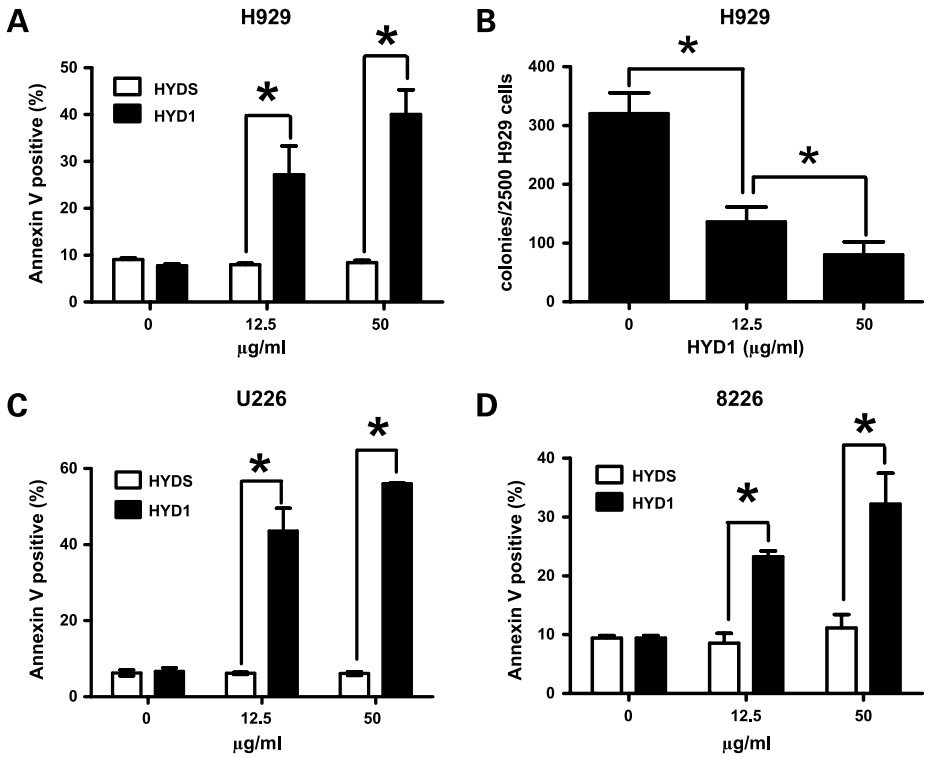


**Figure 2.** HYD1 induces cell death in MM cells. **A, C,** and **D,** H929, U226, and 8226 cells, respectively, were treated with either 0, 12.5, or 50 μg/mL HYD1 or HYDS for 6 h. Annexin V–positive cells were determined by FACS analysis. **B,** H929 cells (2,500) were treated with HYD1 for 2 h before being plated in triplicates in 0.3% agar supplemented with growth media. The number of colonies per 2,500 cells plated was counted after 12 d. Figures, representative of three independent experiments done in triplicate ($n = 9$; *, $P < 0.05$).

Published OnlineFirst August 11, 2009; DOI: 10.1158/1535-7163.MCT-09-0113



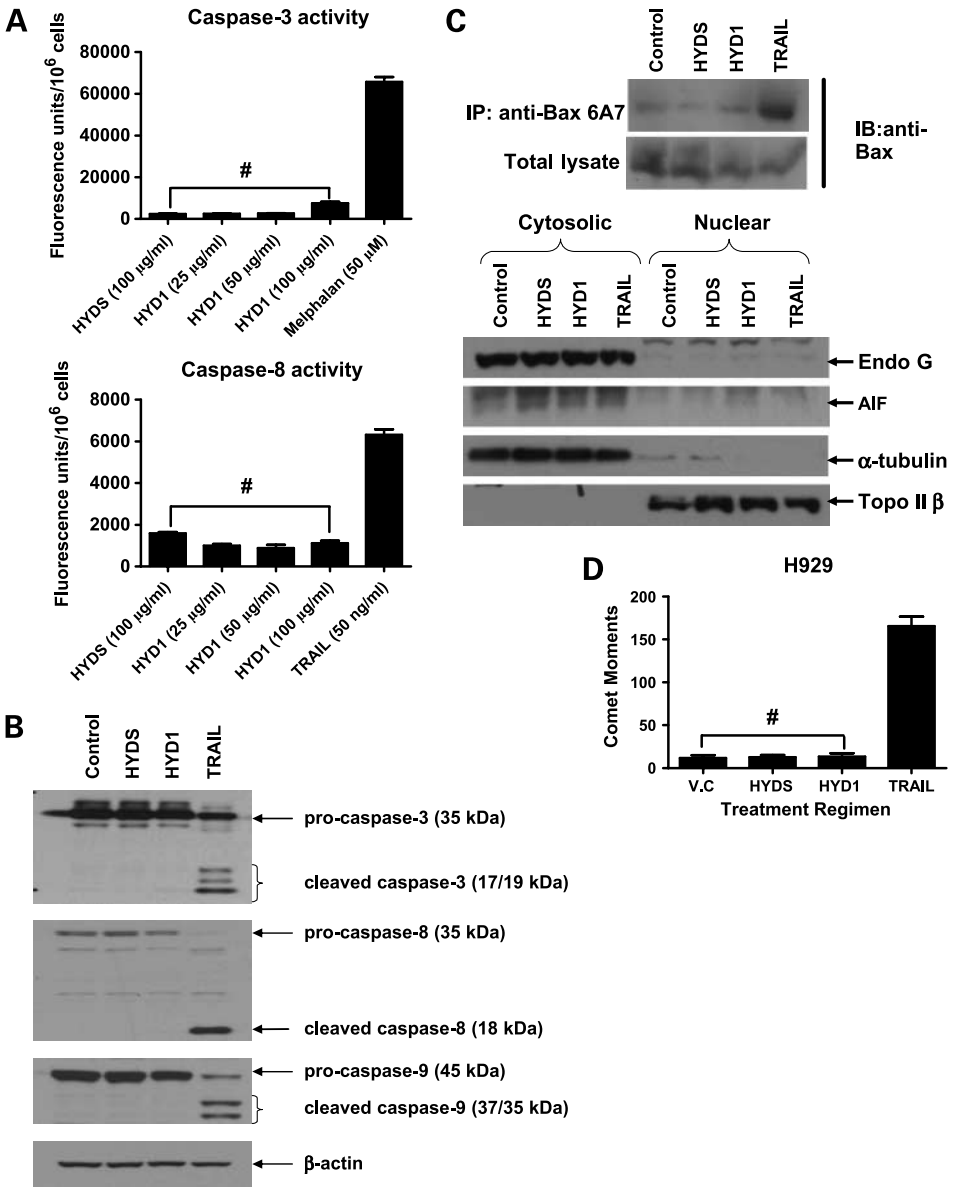


**Figure 3.** HYD1 does not induce apoptotic cell death in MM cells. **A,** H929 ($4 \times 10^5$ cells/mL) were plated in 24-well plates and treated with the indicated concentrations of either HYD1 or HYDS for 6 h, followed by measurement of active caspase-3 and caspase-8 as per manufacturer's instructions ($n = 6$; #, $P > 0.05$). H929 cells ($4 \times 10^5$ cells/mL) were treated for 6 h with either 50 μg/mL of HYD1 and HYDS, or 50 ng/mL of TRAIL. After this, they were subjected to: Western blotting, probing for caspase-3, caspase-8, and caspase-9 (**B**); and immunoprecipitation, for active Bax with the use of 6A7 antibody, and then probing for Bax levels (**C**). Nuclear and cytoplasmic enriched extracts were probed for endonuclease G, apoptosis-inducing factor, α-tubulin, and topoisomerase IIβ; and finally, neutral comet assay was done to measure double-stranded DNA breaks (**D**). The comet moments were calculated by measuring 50 images for each treatment with the use of a charge coupled device (CCD) camera with SmartCapture program ($n = 150$; #, $P > 0.05$). Figures, representative of three independent experiments. TRAIL, tumor necrosis factor–related apoptosis-inducing ligand.

### Autophagy Induced by HYD1 Protects the Cells against Death

Depending on the context, the induction of autophagy has been shown to be associated with cell survival or cell death (22, 23). To determine whether autophagy induced by HYD1 plays a role in cell survival or cell death, we blocked autophagy by two independent methods. We used small interfering RNA targeting Beclin-1, whose expression is required for the formation of preautophagosomal structures, and a pharmacologic approach with the use of 3-methyladenine, a nucleotide derivative and class III PI-3 kinase inhibitor shown to inhibit the earliest stages of autophagosome formation (24, 25). As seen in Fig. 4B and C, both strategies significantly sensitized H929 cells to HYD1-induced cell death. The addition of 3-methyladenine also sensitized 8226 cells to HYD1-induced cell death (see Supplementary Fig. S5). These results indicate that autophagy is an adaptive response and contributes to survival of MM cells after HYD1 treatment. There is a mutual crosstalk between autophagy and apoptosis. It has been reported that certain stimuli can induce cells to undergo autophagic cell death and, upon inhibition of autophagy, under the same stimuli the cells revert to apoptotic cell death (26). To determine whether the increase in cell death observed upon HYD1 treatment under the inhibition of autophagy was due to a switch to apoptotic cell death, we pretreated cells with 3-methyladenine followed by HYD1, and then looked for cleaved caspase-3,

Published OnlineFirst August 11, 2009; DOI: 10.1158/1535-7163.MCT-09-0113



caspase-8, and caspase-9 in cell lysates by Western blot analysis. As shown in Fig. 4D, neither 3-methyladenine, HYD1 alone, nor their combination caused cleavage of caspases. We further validated these findings by repeating the experiment in 8226 cells and found similar results (data not shown). Taken together, these data indicate that inhibition of HYD1-induced autophagy does not sensitize MM cells to undergo caspase-dependent cell death.

### HYD1 Induced Necrotic Cell Death

Major biochemical markers associated with necrotic cell death are the loss of $\Delta\psi_m$ accompanied by loss of total ATP and an increase in ROS production in cells. We found that HYD1 (50 μg/mL) treatment caused a significant loss of $\Delta\psi_m$ in H929 cells (see Fig. 5A). This was accompanied by a 62% decrease in ATP levels (see Fig. 5A). Additionally, HYD1 treatment resulted in a significant increase in ROS production when compared with control cells (see Fig. 5A). Similar results were found in 8226 cells (see Supplementary Fig. S6). All these events occurred rapidly during treatment with HYD1, suggesting that in MM cells HYD1 induces cell death through the necrotic cell death pathway.

### ROS Plays a Role in the Induction of Cell Death and Autophagy in HYD1-Treated MM Cells

ROS has been shown to be an important mediator involved in propagation and execution of necrotic cell death. To investigate whether ROS is the cause of cell death in HYD1-treated cells, we pretreated cells with *N*-acetyl-L-cysteine, a thiol-containing free radical scavenger. The dose of *N*-acetyl-L-cysteine used was shown to be effective in

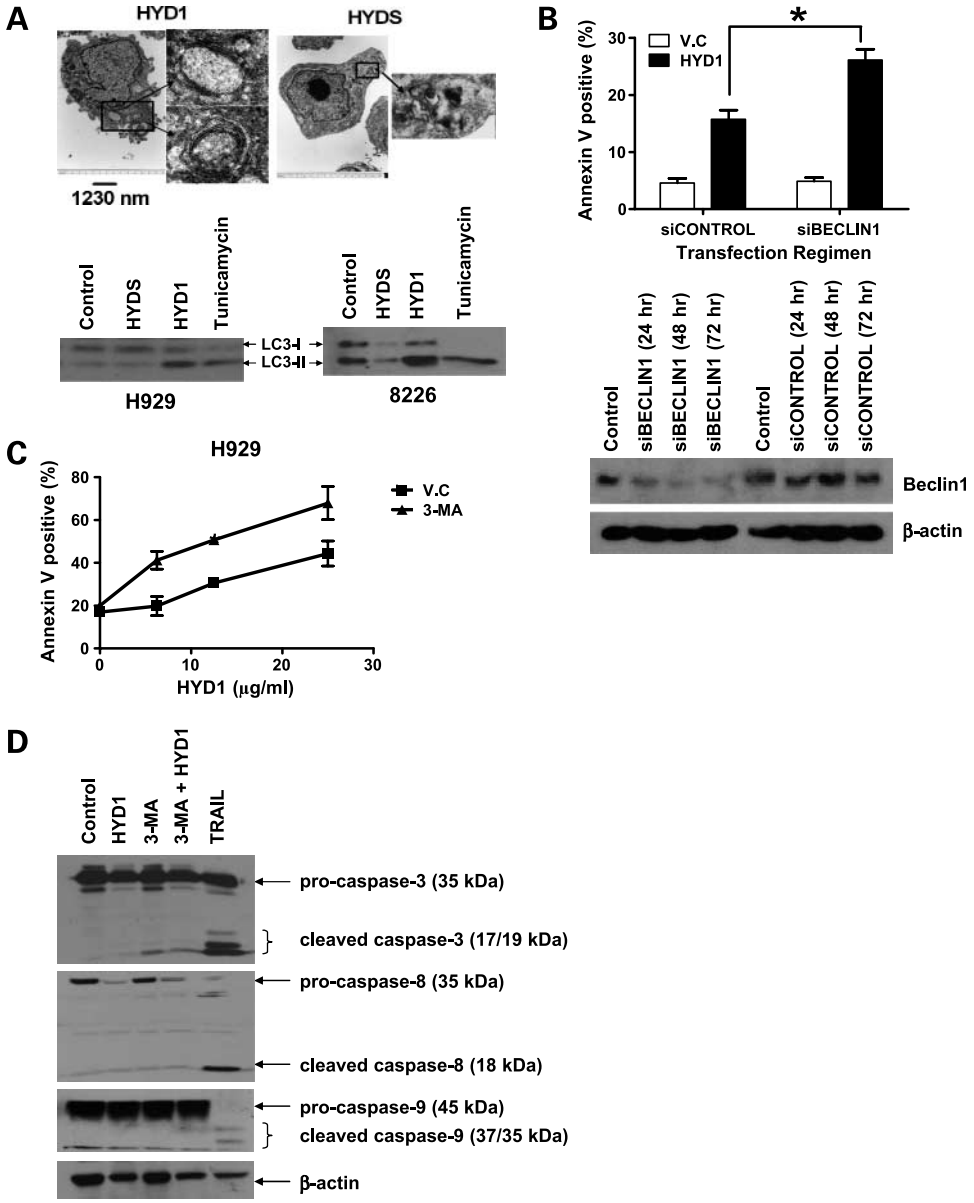


**Figure 4.** HYD1 induces autophagy, which is cytoprotective in MM cells. **A,** H929 cells were treated with either 50 μg/mL HYD1 or HYDS for 4 h, and then processed for electron microscopy as described in Materials and Methods. H929 or 8226 cells were treated with either HYD1 or HYDS (50 μg/mL for H929 and 100 μg/mL for 8226 cells), or 100 μmol/L tunicamycin for 4 h. After treatment, LC3-1 to LC3-II conversion was monitored by Western blot analysis. **B,** H929 cells were transfected with a pool of four siRNA targeting Beclin-1 (siBECLIN-1) or a control off-target siRNA (siCONTROL) with the use of electroporation technique as described in Materials and Methods. Seventy-two hours post transfection, cells were treated for 6 h with HYD1 (50 μg/mL), and cell death was determined by FACS analysis of Annexin V–positive cells ($n = 9$; *, $P < 0.05$). **B,** Western blot analysis showed the reduction of Beclin-1 levels in H929 cells at different time points post transfection. **C,** H929 cells ($4 \times 10^5$ cells/mL) were pretreated with 3-MA (10 mmol/L) for 45 min before the addition of varying concentrations of HYD1. Cell death was determined by FACS analysis of Annexin V–positive cells after 6 h of treatment. ($n = 9$; $P < 0.05$). **D,** H929 cells ($4 \times 10^5$ cells/mL) were pretreated with 3-MA (10 mmol/L) for 45 min before the addition of 50 μg/mL of HYD1 for 6 h and probed for cleaved caspase-3, caspase-9, and caspase-8. Figures, representative of three independent experiments. siRNA, small interfering RNA. 3-MA, 3-methyladenine.

Published OnlineFirst August 11, 2009; DOI: 10.1158/1535-7163.MCT-09-0113



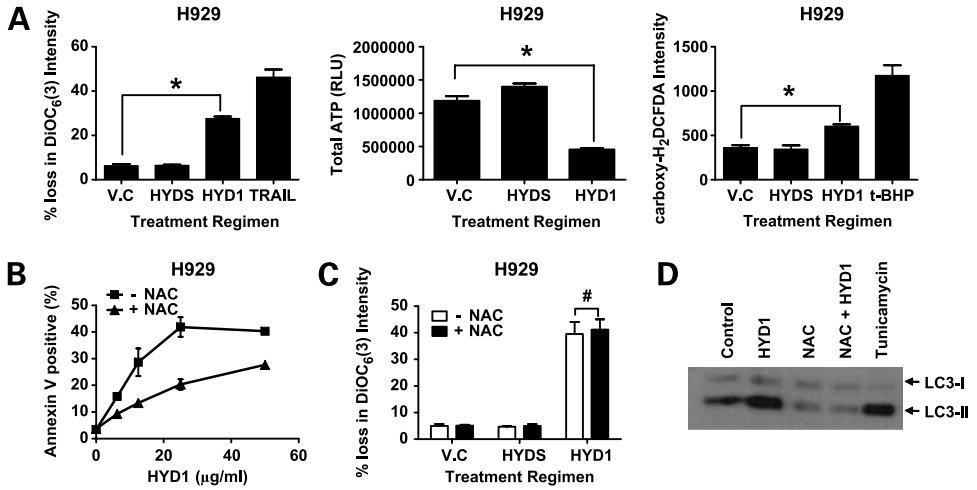


**Figure 5.** HYD1 induces ROS-mediated necrotic cell death in MM cells. **A,** H929 cells ($4 \times 10^5$ cells/mL) were treated for 2 h with HYD1 (50 μg/mL). After treatment, cells were analyzed for loss in $\Delta\psi_m$, total cellular ATP, and ROS production as described in Materials and Methods ($n = 9$; *, $P < 0.05$). **B,** cell death assay was carried out in H929 cells ($4 \times 10^5$ cells/mL) by pretreating with NAC (10 mmol/L) for 30 min, followed by the addition of varying concentrations of HYD1 ($n = 9$; $P < 0.05$). **C,** H929 cells ($4 \times 10^5$ cells/mL) were pretreated with NAC (10 mmol/L) for 30 min before the addition of HYD1 (50 μg/mL) for an additional 4 h. After the treatment, cells were analyzed for loss in $\Delta\psi_m$ ($n = 9$; #, $P > 0.05$). **D,** H929 cells ($4 \times 10^5$ cells/mL) were pretreated with NAC (10 mmol/L) for 30 min before the addition of HYD1 (50 μg/mL) for an additional 4 h. After treatment, LC3-1 to LC3-II conversion was monitored by Western blot analysis. Figures, representative of three independent experiments. NAC, *N*-acetyl-L-cysteine.

inhibiting the production of ROS (Supplementary Fig. S7). As seen in Fig. 5B, *N*-acetyl-L-cysteine partially protects H929 from HYD1-induced cell death. At the highest HYD1 concentration, *N*-acetyl-L-cysteine protected cells from death by 32% in H929 compared with cells treated with HYD1 only. Similar results were found in U226 cells (see Supplementary Fig. S8). These data indicate that ROS plays an important role in inducing necrotic cell death in HYD1-treated MM cells.

Mitochondria are considered the major organelles capable of generating ROS within cells. To determine whether ROS was the cause or the product of loss of $\Delta\psi_m$, we pretreated cells with *N*-acetyl-L-cysteine and followed it by treatment with HYD1. As shown in Fig. 5C, the observed loss in $\Delta\psi_m$ was not reversed by pretreatment with *N*-acetyl-L-cysteine. These data suggest that ROS production lies downstream of disruption of $\Delta\psi_m$.

Finally, oxidative stress has been shown to induce autophagy (22). To investigate whether the autophagy observed in HYD1-treated cells was due to the induction of ROS, we pretreated cells with *N*-acetyl-L-cysteine followed by HYD1 treatment. As shown in Fig. 5D, HYD1 caused a substantial increase in LC3-II formation compared with control cells. The increase in LC3-II was completely reversed by pretreating cells with *N*-acetyl-L-cysteine. Moreover, the addition of *N*-acetyl-L-cysteine reversed basal levels of LC3-II, suggesting that autophagy is driven by endogenous ROS levels in MM cells and may be a general mechanism whereby cancer cells can tolerate high basal levels of ROS typically associated with transformation. Taken together, these data show that HYD1 induces ROS downstream of disruption of mitochondrial membrane potential. Additionally, HYD1 induction of ROS can paradoxically contribute to both cell survival by inducing autophagy and cell death by inducing necrosis in MM cells.

### HYD1 Shows Decreased Potency in Normal Hematopoietic Progenitor Cells and Retains Modest *In vivo* Activity

A colony-forming assay was used to determine whether HYD1 induced cell death in normal hematopoietic cells. As shown in Fig. 6A, HYD1 did not inhibit colony formation of normal $CD34^+$ cells. In addition, we evaluated the toxicity of HYD1 in normal peripheral blood mononuclear cells. As seen in Fig. 6B, 6-hour treatment with increasing concentrations of HYD1 did not induce cell death up to doses of 50 μg/mL in peripheral blood mononuclear cells. Together our data indicate that HYD1 targets MM cells preferentially compared with normal hematopoietic cells.

Finally, we used the SCID-hu model to determine whether HYD1 shows antitumor activity *in vivo*. The SCID-hu model consists of implanting human fetal bone into the mammary mouse fat pad of SCID mice. Circulating κ levels were measured on days 28 (baseline reading before peptide treatment), 35, 42, and 49 by ELISA. Shown in Fig. 6C is the antitumor response of H929-engrafted tumor when mice were given 8 mg/kg i.p. injections daily for 21 days starting on day 28. Mice treated with HYD1 showed a modest but significant reduction in tumor burden compared with control mice. In these experiments, no overt toxicity or weight loss was noted in HYD1 treated animals. Further studies are warranted to determine whether the *in vivo* activity of HYD1 can be improved by using PEGylation or cyclization strategies to increase the bioavailability and, potentially, the antitumor activity of HYD1. Represented in Fig. 6D is our working model of the mechanism of action associated with HYD1-induced

Published OnlineFirst August 11, 2009; DOI: 10.1158/1535-7163.MCT-09-0113



cell death. Based on our results, further studies are warranted to determine the upstream targets causative for HYD1-induced depolarization of the mitochondrial membrane potential.

## Discussion

HYD1 was previously identified with the use of a combinatorial peptide synthesis in combination with an adhesion-based screen (15). HYD1 has been previously shown to block random haptotactic migration and inhibit invasion of epithelial prostate carcinoma cells on laminin-5 (laminin-332; ref. 8). These studies showed that HYD1 interacted with α6 and α3 integrins (laminin receptors) on the tumor cell surface, and blocked adhesion while inducing an elevation of laminin-5 (laminin-332)–dependent intracellular signaling, including focal adhesion kinase, mitogen-activated protein kinase, and extracellular signal-regulated kinase (8). Currently, it is unclear if cell death associated with HYD1 treatment is due to direct binding of the α-subunit or whether HYD1 interacts with an integrin-binding death-inducing partner, associated with specific α-subunits, in a multiprotein complex. It must be noted that a β1-blocking antibody does not induce cell death in MM cells (data not shown), indicating that HYD1 has unique binding properties and may indeed act as an agonist for inducing cell death. Further studies are warranted to validate HYD1 target(s) associated with the induction of cell death.

In addition to blocking cell adhesion and reversing resistance associated with the HS-5 bone marrow stroma coculture model, we have shown in this report for the first time that HYD1, a D–amino acid peptide, induces cell death as a single agent in MM cells grown *in vitro*. More importantly, HYD1 treatment was found to be less toxic to $CD34^+$ progenitor cells and peripheral blood mononuclear cells compared with MM cells. We further show that HYD1-induced cell death in MM cells showed markers that are characteristic of necrosis because cell death was accompanied by loss of $\Delta\psi_m$, decrease in total cellular ATP, and a significant increase in ROS. Also, HYD1-induced cell death could be partially reversed by pretreating cells with the ROS scavenger *N*-acetyl-L-cysteine. Another interesting finding in our study is that the oxidative stress induced by HYD1 resulted in the initiation of an autophagic pathway, which paradoxically protected the cells against HYD1-induced cell death.

Caspase-dependent apoptosis is induced through two major pathways: one involves the death receptor, called the extrinsic pathway, and utilizes caspase-8; another is the intrinsic pathway, involving the mitochondria and mediated by caspase-9 (27, 28). Both of these pathways converge on caspase-3 activation, eventually resulting in

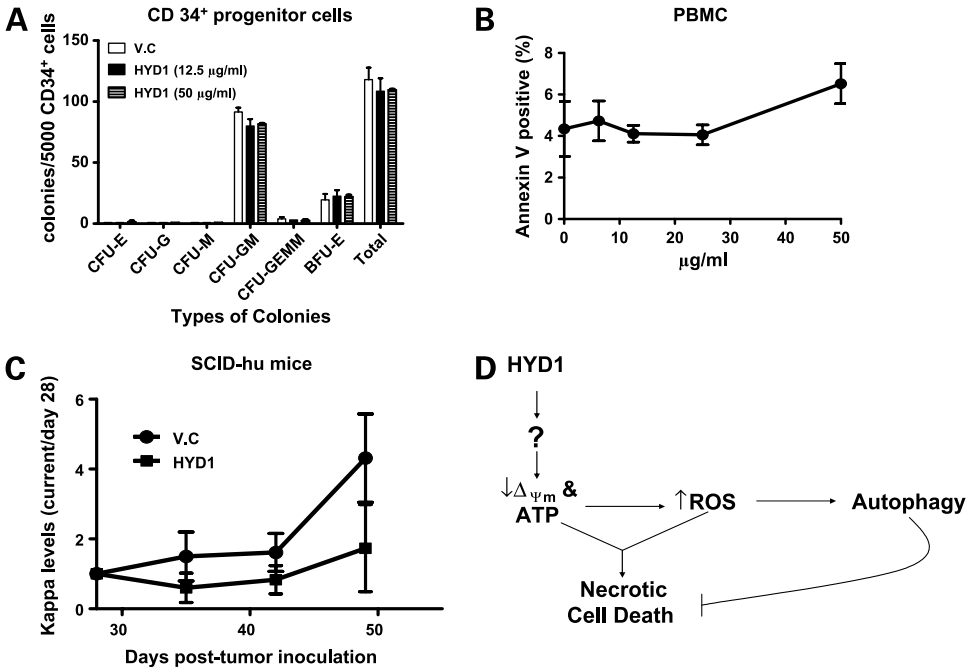


**Figure 6.** HYD1 lacks activity in normal hematopoietic cells and shows antitumor activity *in vivo*. **A,** $CD34^+$ cells were isolated from PBMC of healthy donors and subjected to colony-forming assay as described in Materials and Methods. The number of colonies per 5,000 cells was counted at the end of day 12. Experiments were done twice in duplicates. **B,** PBMCs were isolated by density gradient centrifugation with the use of Ficoll-Paque. Isolated PBMCs ($4 \times 10^5$ cells/mL) were plated in 24-well plates and treated with the indicated concentrations of HYD1 for 6 h, followed by measurement of dead cells by FACS analysis of Annexin V–positive cells. **C,** tumor burden in the SCID-Hu model was measured by circulating κ levels by ELISA. On day 28 (before drug treatment), measurements were recorded for each individual mouse, and subsequent values obtained weekly are represented as a ratio of day 28 (day X/day28). HYD1 was given i.p. at 8 mg/kg daily for 21 d (starting day 28). $n = 5$ for vehicle control (V.C.); $n = 4$ for HYD1-treated mice ($P < 0.05$). **D,** a representative model depicting the putative mechanism of action of HYD1 in MM cells. PBMC, peripheral blood mononuclear cell.

Published OnlineFirst August 11, 2009; DOI: 10.1158/1535-7163.MCT-09-0113



DNA fragmentation (29). In our study, HYD1 did not activate either the intrinsic or the extrinsic pathway of apoptosis, as confirmed by measuring three different end points: (*a*) absence of cleaved caspases in HYD1-treated cells by Western blotting, (*b*) absence of caspase activity in HYD1-treated cells by substrate cleavage, and (*c*) failure of zVAD-fmk, a pan caspase inhibitor, to block HYD1-induced cell death as ascertained by Annexin V–FITC/PI binding studies.

DNA fragmentation can also occur through the mitochondrial death effector proteins apoptosis-inducing factor and endonuclease G. Under some cytotoxic stimuli, both apoptosis-inducing factor and endonuclease G are released from the mitochondria and translocate to the nucleus where they cause large-scale DNA fragmentation (29, 30). In our study, HYD1 did not trigger the translocation of apoptosis-inducing factor and endonuclease G to the nucleus. This observation was consistent with the finding that HYD1 treatment did not activate Bax or caspases. Importantly, these studies were done in cell lines capable of activating caspases. Thus, in the cell lines tested, HYD1 activates caspase-independent cell death not as a default pathway but rather as a primary mode of cell death.

Necrosis is the consequence of extensive crosstalk between several biochemical and molecular events. Currently, there is no single well-described signaling cascade to define necrotic cell death (for review, see ref. 31). Similarly in our study, we show three different biochemical events, namely loss of $\Delta\psi$m, decrease in cellular ATP, and increased production of ROS, as evidence for the HYD1-induced necrotic cell death. Further studies are warranted to determine the mechanism of HYD1-induced loss of $\Delta\psi_m$ without activation of Bax, release of apoptosis-inducing factor and endonuclease G, or activation of caspases. Likely candidates for the cause of HYD1-induced loss of $\Delta\psi_m$ may include activated Bcl-2 family member BNIP3, cyclophilin D, or calcium overload, all of which, either alone or in concert, are reported to cause a decrease in mitochondrial membrane potential without release of intermembrane space proteins (6, 32, 33). Loss of $\Delta\psi_m$ can lead to mitochondrial dysfunction, resulting in a breakdown of the respiratory chain and the overproduction of ROS concomitant with uncontrolled hydrolysis of ATP, ultimately leading to necrotic cell death (34). Interestingly, in our study ROS seems to be a major player in the induction of necrotic cell death, because we could partially reverse HYD1-induced cell death by pretreating the cells with a ROS scavenger, *N*-acetyl-L-cysteine.

In the present study, in addition to necrotic cell death, we show that HYD1 treatment resulted in a manifestation of morphologic and biochemical markers that are indicative of autophagy. These markers included the extensive formation of double membrane–containing vesicles and lipidation of LC3. Although autophagy is a ubiquitous process in mammalian cells that contributes to the routine turnover of cytoplasmic components in case of cellular stress, autophagy can act as a defense mechanism involving the removal and recycling of damaged proteins and organelles by delivering them to lysosomes (for review, see ref. 35). In the present study, we show that an increase in ROS in HYD1-treated cells results in the induction of autophagy. This observation is consistent with previous reports showing that elevated ROS levels induce autophagy through the oxidation of a cysteine residue on Atg4 (36).

In summary, these studies show that although HYD1 can block $\alpha4\beta1$ integrin–dependent binding of MM cells to fibronectin, HYD1 also induces cell death *in vitro.* Although the *in vivo* activity was modest, we are currently pursuing strategies, such as PEGylation and cyclization, that will increase the bioavailability of the peptide *in vivo*. Importantly, HYD1 increased the levels of melphalan-specific cell death and reversed resistance to melphalan-associated cell death when coculturing myeloma cells with the bone marrow stroma cell line HS-5. Together these data suggest that HYD1 may be an attractive agent to combine with agents that (*a*) target the apoptotic machinery and (*b*) are resistant in a bone marrow stroma coculture model system. Mechanistically, HYD1 treatment leads to the loss of $\Delta\psi_m$ and a decrease in cellular ATP, resulting in an increase in ROS production. All of these three biochemical events ultimately lead to necrotic cell death in MM cells. Moreover, we anticipate that HYD1 will prove to be an important tool to dissect the molecular pathway of caspase-independent cell death, and allow for investigations for deciphering crosstalk between apoptotic and nonapoptotic cell death pathways. Finally, drug resistance is often associated with an imbalance in proapoptotic and antiapoptotic mediators, with the net result favoring cell survival. Thus, agents, such as HYD1, that preferentially target alternative cell death pathways may provide an ideal strategy for developing combination therapies to eliminate subpopulations of cells resistant to apoptotic cell death.

## Disclosure of Potential Conflicts of Interest

L. Hazelhurst, A.E. Cress, K. Lam, and W.S. Dalton have no current financial interest, but have submitted a patent pertaining to the anti-tumor activity of HYD1.

### References

**1.** Hu X, Xuan Y. Bypassing cancer drug resistance by activating multiple death pathways-a proposal from the study of circumventing cancer drug resistance by induction of necroptosis. Cancer Lett 2008;259:127–37.

**2.** Galluzzi L, Maiuri MC, Vitale I, et al. Cell death modalities: classification and pathophysiological implications. Cell Death Differ 2007;14:1237–43.

**3.** Reed JC, Pellecchia M. Apoptosis-based therapies for hematologic malignancies. Blood 2005;106:408–18.

**4.** Degenhardt K, Mathew R, Beaudoin B, et al. Autophagy promotes tumor cell survival and restricts necrosis, inflammation, and tumorigenesis. Cancer Cell 2006;10:51–64.

**5.** Shimizu S, Kanaseki T, Mizushima N, et al. Role of Bcl-2 family proteins in a non-apoptotic programmed cell death dependent on autophagy genes. Nat Cell Biol 2004;6:1221–8.

**6.** Brookes PS, Yoon Y, Robotham JL, Anders MW, Sheu SS. Calcium, ATP, and ROS: a mitochondrial love-hate triangle. Am J Physiol 2004; 287:C817–33.

**7.** Leist M, Single B, Castoldi AF, Kuhnle S, Nicotera P. Intracellular adenosine triphosphate (ATP) concentration: a switch in the decision between apoptosis and necrosis. J Exp Med 1997;185:1481–6.

**8.** Sroka TC, Pennington ME, Cress AE. Synthetic D-amino acid peptide inhibits tumor cell motility on laminin-5. Carcinogenesis 2006;27: 1748–57.

**9.** Damiano JS, Cress AE, Hazlehurst LA, Shtil AA, Dalton WS. Cell adhesion mediated drug resistance (CAM-DR): role of integrins and resistance to apoptosis in human myeloma cell lines. Blood 1999;93:1658–67.

**10.** Hazlehurst LA, Damiano JS, Buyuksal I, Pledger WJ, Dalton WS. Adhesion to fibronectin via β1 integrins regulates p27kip1 levels and contributes to cell adhesion mediated drug resistance (CAM-DR). Oncogene 2000;19:4319–27.

**11.** Nefedova Y, Landowski TH, Dalton WS. Bone marrow stromal-derived soluble factors and direct cell contact contribute to *de novo* drug resistance of myeloma cells by distinct mechanisms. Leukemia 2003;17:1175–82.

**12.** Hazlehurst LA, Valkov N, Wisner L, et al. Reduction in drug-induced DNA double-strand breaks associated with β1 integrin-mediated adhesion correlates with drug resistance in U937 cells. Blood 2001;98:1897–903.

**13.** Turner JG, Engel R, Derderian JA, Jove R, Sullivan DM. Human topoisomerase IIα nuclear export is mediated by two CRM-1-dependent nuclear export signals. J Cell Sci 2004;117:3061–71.

**14.** Zhu K, Gerbino E, Beaupre DM, et al. Farnesyltransferase inhibitor R115777 (Zarnestra, tipifarnib) synergizes with paclitaxel to induce apoptosis and mitotic arrest and to inhibit tumor growth of multiple myeloma cells. Blood 2005;105:4759–66.

**15.** DeRoock IB, Pennington ME, Sroka TC, et al. Synthetic peptides inhibit adhesion of human tumor cells to extracellular matrix proteins. Cancer Res 2001;61:3308–15.

**16.** Arnoult D, Gaume B, Karbowski M, Sharpe JC, Cecconi F, Youle RJ. Mitochondrial release of AIF and EndoG requires caspase activation downstream of Bax/Bak-mediated permeabilization. EMBO J 2003;22:4385–99.

**17.** van Loo G, Schotte P, van Gurp M, et al. Endonuclease G: a mitochondrial protein released in apoptosis and involved in caspase-independent DNA degradation. Cell Death Differ 2001;8:1136–42.

**18.** Wang X, Yang C, Chai J, Shi Y, Xue D. Mechanisms of AIF-mediated apoptotic DNA degradation in Caenorhabditis elegans. Science 2002;298:1587–92.

**19.** Hsu YT, Youle RJ. Nonionic detergents induce dimerization among members of the Bcl-2 family. J Biol Chem 1997;272:13829–34.

**20.** Enari M, Sakahira H, Yokoyama H, Okawa K, Iwamatsu A, Nagata S. A caspase-activated DNase that degrades DNA during apoptosis, and its inhibitor ICAD. Nature 1998;391:43–50.

**21.** Mizushima N, Yoshimori T. How to interpret LC3 immunoblotting. Autophagy 2007;3:542–5.

**22.** Chen Y, McMillan-Ward E, Kong J, Israels SJ, Gibson SB. Oxidative stress induces autophagic cell death independent of apoptosis in transformed and cancer cells. Cell Death Differ 2008;15:171–82.

**23.** Ogata M, Hino S, Saito A, et al. Autophagy is activated for cell survival after endoplasmic reticulum stress. Mol Cell Biol 2006;26:9220–31.

**24.** Mizushima N, Yamamoto A, Hatano M, et al. Dissection of autophagosome formation using Apg5-deficient mouse embryonic stem cells. J Cell Biol 2001;152:657–68.

**25.** Seglen PO, Gordon PB. 3-Methyladenine: specific inhibitor of autophagic/lysosomal protein degradation in isolated rat hepatocytes. Proc Natl Acad Sci U S A 1982;79:1889–92.

**26.** Boya P, Gonzalez-Polo RA, Casares N, et al. Inhibition of macroautophagy triggers apoptosis. Mol Cell Biol 2005;25:1025–40.

**27.** Li H, Zhu H, Xu CJ, Yuan J. Cleavage of BID by caspase 8 mediates the mitochondrial damage in the Fas pathway of apoptosis. Cell 1998;94:491–501.

**28.** Li P, Nijhawan D, Budihardjo I, et al. Cytochrome c and dATP-dependent formation of Apaf-1/caspase-9 complex initiates an apoptotic protease cascade. Cell 1997;91:479–89.

**29.** Liu X, Zou H, Slaughter C, Wang X. DFF, a heterodimeric protein that functions downstream of caspase-3 to trigger DNA fragmentation during apoptosis. Cell 1997;89:175–84.

**30.** Susin SA, Lorenzo HK, Zamzami N, et al. Molecular characterization of mitochondrial apoptosis-inducing factor. Nature 1999;397:441–6.

**31.** Festjens N, Vanden Berghe T, Vandenabeele P. Necrosis, a well-orchestrated form of cell demise: signalling cascades, important mediators and concomitant immune response. Biochim Biophys Acta 2006;1757:1371–87.

**32.** Nakagawa T, Shimizu S, Watanabe T, et al. Cyclophilin D-dependent mitochondrial permeability transition regulates some necrotic but not apoptotic cell death. Nature 2005;434:652–8.

**33.** Vande Velde C, Cizeau J, Dubik D, et al. BNIP3 and genetic control of necrosis-like cell death through the mitochondrial permeability transition pore. Mol Cell Biol 2000;20:5454–68.

**34.** Lemasters JJ, Nieminen AL, Qian T, et al. The mitochondrial permeability transition in cell death: a common mechanism in necrosis, apoptosis and autophagy. Biochim Biophys Acta 1998;1366:177–96.

**35.** Klionsky DJ. Autophagy: from phenomenology to molecular understanding in less than a decade. Nat Rev 2007;8:931–7.

**36.** Scherz-Shouval R, Shvets E, Fass E, Shorer H, Gil L, Elazar Z. Reactive oxygen species are essential for autophagy and specifically regulate the activity of Atg4. EMBO J 2007;26:1749–60.

AACR American Association for Cancer Research

Molecular Cancer Therapeutics

# HYD1-induced increase in reactive oxygen species leads to autophagy and necrotic cell death in multiple myeloma cells

Rajesh R. Nair, Michael F. Emmons, Anne E. Cress, et al.

*Mol Cancer Ther* 2009;8:2441-2451. Published OnlineFirst August 11, 2009.